OXFORD

JNCI J Natl Cancer Inst (2020) 112(7): djz213

doi: 10.1093/jnci/djz213
First published online October 30, 2019
Article

ARTICLE

Immune Checkpoint Profiles in Luminal B Breast Cancer (Alliance)

Meenakshi Anurag, Mayanne Zhu, Chen Huang, Suhas Vasaikar, Junkai Wang, Jeremy Hoog, Samantha Burugu, Dongxia Gao, Vera Suman, Xiang H. Zhang, Bing Zhang, Torsten Nielsen, Matthew J. Ellis

See the Notes section for the full list of authors' affiliations.
Correspondence to: Meenakshi Anurag, PhD, Lester and Sue Smith Breast Center, Baylor College of Medicine, Houston, TX 77030 (e-mail: anurag@bcm.edu) and Matthew J. Ellis, MB, BChir, PhD, FRCP, Lester and Sue Smith Breast Center, Baylor College of Medicine, Houston, TX 77030 (e-mail: matthew.ellis@bcm.edu).

Abstract

Background: Unlike estrogen receptor (ER)-negative breast cancer, ER-positive breast cancer outcome is less influenced by lymphocyte content, indicating the presence of immune tolerance mechanisms that may be specific to this disease subset.
Methods: A supervised analysis of microarray data from the ACOSOG Z1031 (Alliance) neoadjuvant aromatase inhibitor (AI) trial identified upregulated genes in Luminal (Lum) B breast cancers that correlated with AI-resistant tumor proliferation (percentage of Ki67-positive cancer nuclei, Pearson $r > 0.4$) (33 cases Ki67 > 10% on AI) vs LumB breast cancers that were more AI sensitive (33 cases Ki67 < 10% on AI). Overrepresentation analysis was performed using WebGestalt. All statistical tests were two-sided.
Results: Thirty candidate genes positively correlated ($r \geq 0.4$) with AI-resistant proliferation in LumB and were upregulated greater than twofold. Gene ontologies identified that the targetable immune checkpoint (IC) components *IDO1*, *LAG3*, and *PD1* were overrepresented resistance candidates ($P \leq .001$). High *IDO1* mRNA was associated with poor prognosis in LumB disease (Molecular Taxonomy of Breast Cancer International Consortium, hazard ratio = 1.43, 95% confidence interval = 1.04 to 1.98, $P = .03$). IDO1 also statistically significantly correlated with STAT1 at protein level in LumB disease (Pearson $r = 0.74$). As a composite immune tolerance signature, expression of IFN-γ/STAT1 pathway components was associated with higher baseline Ki67, lower estrogen, and progesterone receptor mRNA levels and worse disease-specific survival ($P = .002$). In a tissue microarray analysis, IDO1 was observed in stromal cells and tumor-associated macrophages, with a higher incidence in LumB cases. Furthermore, *IDO1* expression was associated with a macrophage mRNA signature (M1 by CIBERSORT Pearson $r = 0.62$) and by tissue microarray analysis.
Conclusions: Targetable IC components are upregulated in the majority of endocrine therapy–resistant LumB cases. Our findings provide rationale for IC inhibition in poor-outcome ER-positive breast cancer.

ER-positive (ER+) breast cancer represents approximately 75% of breast cancer cases. Prognosis can be classified using a variety of gene expression signatures, but a simple definition has two intrinsic subtypes: Luminal (Lum) A and LumB. LumA tumors have a lower proliferation rate and a more favorable prognosis, whereas LumB tumors exhibit higher grade, lower ER; greater proliferation rates; and worse survival. The LumB subtype accounts for nearly 40% of node-negative early-stage breast cancers (1) and requires focused investigation to identify new therapeutic options.

Standard-of-care endocrine therapy (ET), mostly tamoxifen or aromatase inhibition with or without ovarian suppression, dramatically improves the outcome for ER+ breast cancers (2–4). However, neoadjuvant ET studies demonstrate that

Received: February 4, 2019; **Revised:** September 12, 2019; **Accepted:** October 25, 2019

approximately one-third of cases fail to suppress the Ki67 index (percentage of Ki67-positive cancer nuclei) less than 10% within 2 to 4 weeks of ET initiation, indicating tumor proliferation that is decoupled from ER regulation (5). Patients with intrinsically ET-resistant tumors experience early mortality that is not explained by mutations in ER or mitogen-activated protein kinase pathways, which are more typical of tumors that relapse after years of ET exposure (6,7). Our group recently identified defects in single-stranded DNA damage repair as a driver of intrinsic ET resistance (8,9). Because defects in DNA damage repair lead to higher somatic mutation burden and greater immunogenicity (10), we postulated that aggressive LumB ET-resistant tumors must evolve immune tolerance mechanisms that allow disease progression.

To investigate ET resistance in LumB breast cancer, transcriptome-wide unbiased profiling was employed to identify the genes that associate with poor neoadjuvant ET response and demonstrate upregulation in LumB vs LumA disease. This analysis identified immune checkpoint (IC) components that were further explored in independent datasets as well as by tissue microarray analysis.

Methods

Patient Datasets and Analysis

Microarray data, clinical annotations, and 50-gene predictor of breast cancer subtype (PAM50 calls) from patients on neoadjuvant aromatase inhibitor (AI) trials ACOSOG Z031 (Alliance) and Preoperative Letrozole (POL) were used with permission from the Alliance for Clinical Trials in Oncology (ACOSOG is now part of Alliance). Each participant signed an institutional review board–approved, protocol-specific, informed consent document for use of their samples in accordance with federal and institutional guidelines. Expression data on POL and Z1031 cases can be accessed via GSE29442, GSE35186, GSE87411, and GSE136644. The sample acquisition, data, and conduct of the study have been previously reported (8). For these analyses, samples from biopsies taken before treatment are referred to as baseline and those taken at approximately 4 weeks of AI treatment are referred to as on-treatment samples. The entire dataset from the POL and Z1031 cohort is collectively referred to as Z1031 henceforth and was used as the discovery cohort. The microarray data comprise expression for 15 500 genes for 428 samples, of which 66 were annotated as LumB by PAM50 subtyping. A standard cutoff of median expression value of candidate genes in the study was used to identify "high" (greater than median) and "low" (equal to or less than median) sets. Tumors with on-treatment Ki67 (by Immunohistochemistry (IHC)) greater than 10% were categorized to be ET-resistant cases (n = 33), and cases with lower Ki67 were categorized as ET-sensitive cases (n = 33; Supplementary Figure 1 available online).

Statistical Analysis

In an unbiased analysis, mRNA expression data for approximately 15 500 genes across the 66 LumB subset were used to identify genes for which the expression correlated positively with proliferation marker Ki67 (post-AI treatment) and were upregulated (greater than twofold) in ET-resistant cases compared with ET-sensitive cases (Figure 1). Pearson's correlation was performed individually on the log-transformed normalized data for approximately 15 500 genes using automated script in R. Multiple testing adjustment was achieved via the Benjamini-Hochberg false discovery rate (FDR). Correlations with a coefficient of at least 0.4 were considered to be positively correlated. Detailed statistics are reported in Supplementary Table 1 (available online). Mean expression for each of the approximately 15 500 was calculated in ET-resistant and sensitive tumor sets separately; if the fold difference was greater than two in resistant tumors, then the gene was a candidate for upregulation in ET-resistant tumors. Overrepresentation analysis using WebGestalt (11,12) on the resulting set of 30 genes was performed to identify statistically significantly represented gene ontologies (nonredundant biological processes ranging in size range from five to 250) at FDR less than or equal to 20%. Detailed statistics on overrepresented ontologies are reported in Supplementary Table 2 (available online).

To achieve orthogonal validation of genes associated with ET-resistant LumB disease in Molecular Taxonomy of Breast Cancer International Consortium (METABRIC) and The Cancer Genome Atlas (TCGA), RNA expression datasets and survival data were examined using Kaplan-Meier estimates (13) and a log-rank test. Proportional hazards were determined using Cox regression model (14). Proportion hazards were considered statistically significant with a P value less than .05. Amplification and methylation data for TCGA samples were obtained from Wanderer (15). Protein levels and correlations for TCGA samples using Clinical Proteome Tumor Analysis Consortium (CPTAC) data were obtained from LinkedOmics (16,17).

Comparisons between groups were performed using the Wilcoxon rank-sum test for continuous variables, Wilcoxon signed-ranked test for paired data, and Fisher exact test for categorical variables. Disease specific survival (DSS) was defined as the time from date of diagnosis to date of death attributed to breast cancer. All statistical tests were two-sided, and differences were considered statistically significant when P was less than .05.

Tissue Microarray Analysis

Detailed methods are provided in the Supplementary Methods (available online).

Results

High Immune Tolerance Signatures in LumB Tumors Resistant to ET

An unbiased analysis was conducted using Z1031 baseline tumor mRNA profiling data to identify genes that were upregulated in ET-resistant LumB breast cancer and, as a marker for ET sensitivity, also correlated with Ki67 values determined approximately 4 weeks after ET was initiated (Figure 1A). This yielded a set of 30 candidate genes that were associated with ET resistance in LumB disease with an FDR coefficient greater than or equal to 0.4 (Figure 1B). Consistent with our earlier reports (8,9,18), the mismatch repair gene *MLH1* was one of the highly downregulated genes in the ET-resistant set of LumB cases (Figure 1B). Application of WebGestalt indicated that candidate genes were overrepresented in immune tolerance biological processes (Figure 1C), namely, tolerance induction ($P < .001$) and negative regulation of T-cell activation ($P = .001$). The four genes constituting these processes were *IDO1*, *PD1*, *LAG3*, and *INPPD5* (*SHIP1*), of which the first three are targetable IC components (19,20).

ARTICLE

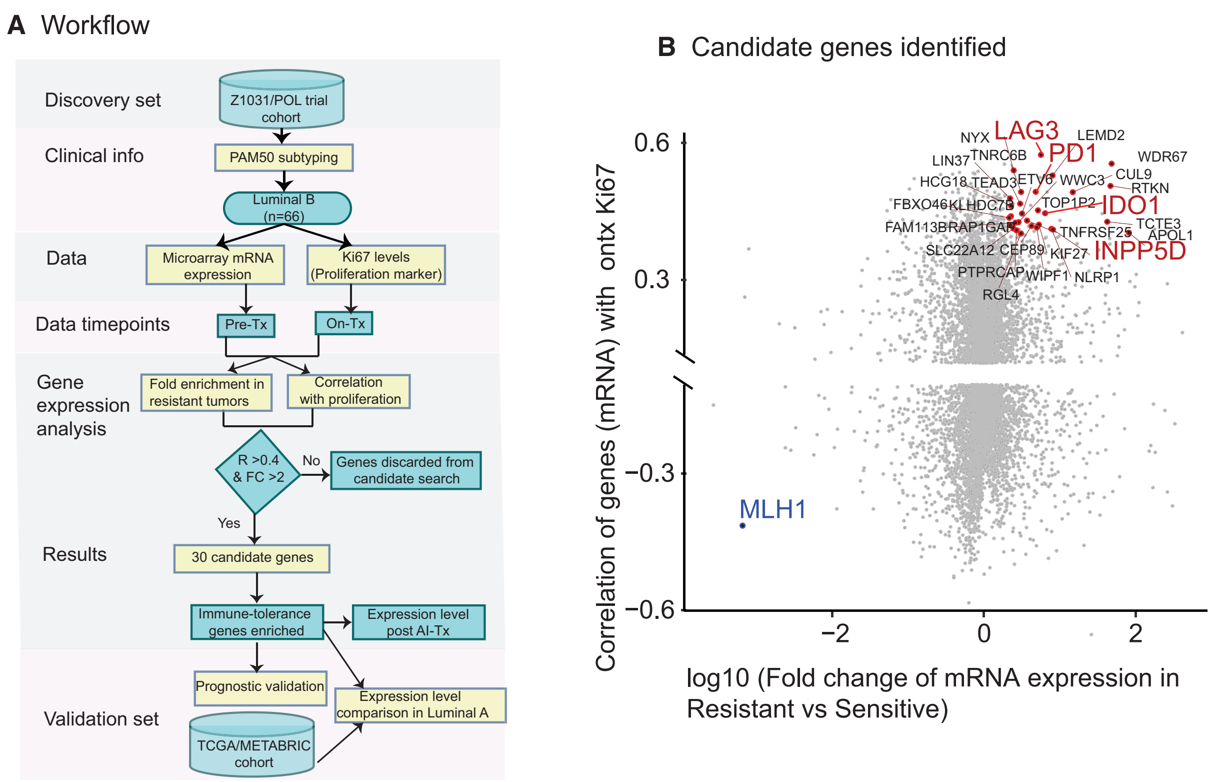

C Enriched ontologies

Ontology name	No. of genes in ontology	No. of candidate genes in GO	*P*-value	Contributing genes
Tolerance induction	21	2	<.001	*IDO1, PDCD1*
Hippo signaling	38	2	.001	*WWC3, TEAD3*
Negative regulation Of cell activation	174	3	.001	*IDO1, LAG3, INPP5D*
Cortical cytoskeleton Organization	43	2	.001	*RTKN, WIPF1*

D Association with prognosis (TCGA)

Genes	Luminal A (n=263) HR (95% CI)	Luminal A (n=263) Log-rank *P*-value	Luminal B (n=106) HR (95% CI)	Luminal B (n=106) Log-rank *P*-value
IDO1	0.89 (0.23-3.41)	.97	7.35 (0.87-61.88)	.03
LAG3	1.53 (0.44-5.32)	.5	6.86 (0.82-57.35)	.04
PDCD1	0.92 (0.27-3.15)	.89	3.46 (0.65-18.42)	.12
INPP5D	1.39 (0.42-4.62)	.59	1.99 (0.43-9.35)	.37

Figure 1. Candidate genes identification. **A)** Schema depicting the approach taken to identify genes that correlate with Ki67 and are overexpressed in endocrine therapy (ET)-resistant breast cancer samples, where R stands for Pearson correlation coefficient and FC for fold change. **B)** Scatterplot showing high (**red**) and low (**blue**) expressed genes, which positively or negatively correlate with tumor proliferation on aromatase inhibitor (AI) treatment, respectively. **C)** Table showing gene ontologies enriched in genes (candidate genes) that were highly expressed in treatment-resistant cases and also correlated with high proliferation on treatment. **D)** Table showing hazard ratio and log-rank P value for immune tolerance genes from candidate list in ER-positive cases (TCGA). All the tests were two-sided.

IDO1 in Poor-Prognosis LumB Breast Cancer

Our discovery analyses suggested higher expression of selected IC genes in LumB ET-resistant cases. For validation, we examined both the TCGA and METABRIC datasets. As anticipated from the Z1031 analysis, IDO1 and LAG3 mRNA levels in TCGA were associated with poor survival, specifically in LumB cases (Figure 1D). High levels of IDO1 mRNA were particularly associated with poor DSS in LumB cases (hazard ratio = 7.35, 95% confidence interval = 0.87 to 61.88), and hence this gene was prioritized for detailed further analyses. When LumA and LumB cases were contrasted (Figure 2A), higher IDO1 mRNA were observed in LumB cases (median [SD] LumA = −0.88 [1.47] vs LumB = −0.51 [1.70], P = .01). This was confirmed by proteomics data (21) from TGCA samples (Figure 2A; median [SD] LumA = −0.34 [0.72] vs LumB = 0.04 [0.93], P = .04). A higher incidence of early death less than 5 years vs greater than 5 years in LumB cases was a clinically important feature of high IDO1 mRNA levels (P = .01; Supplementary Figure 2A, available online). An association between high IDO1 mRNA levels and poor DSS was also observed in METABRIC, specifically in LumB cases (hazard ratio = 1.43, 95% confidence interval = 1.04 to 1.98, P = .03; Figure 2D). A multivariable analysis was conducted in the METABRIC dataset to determine if the prognostic influence of

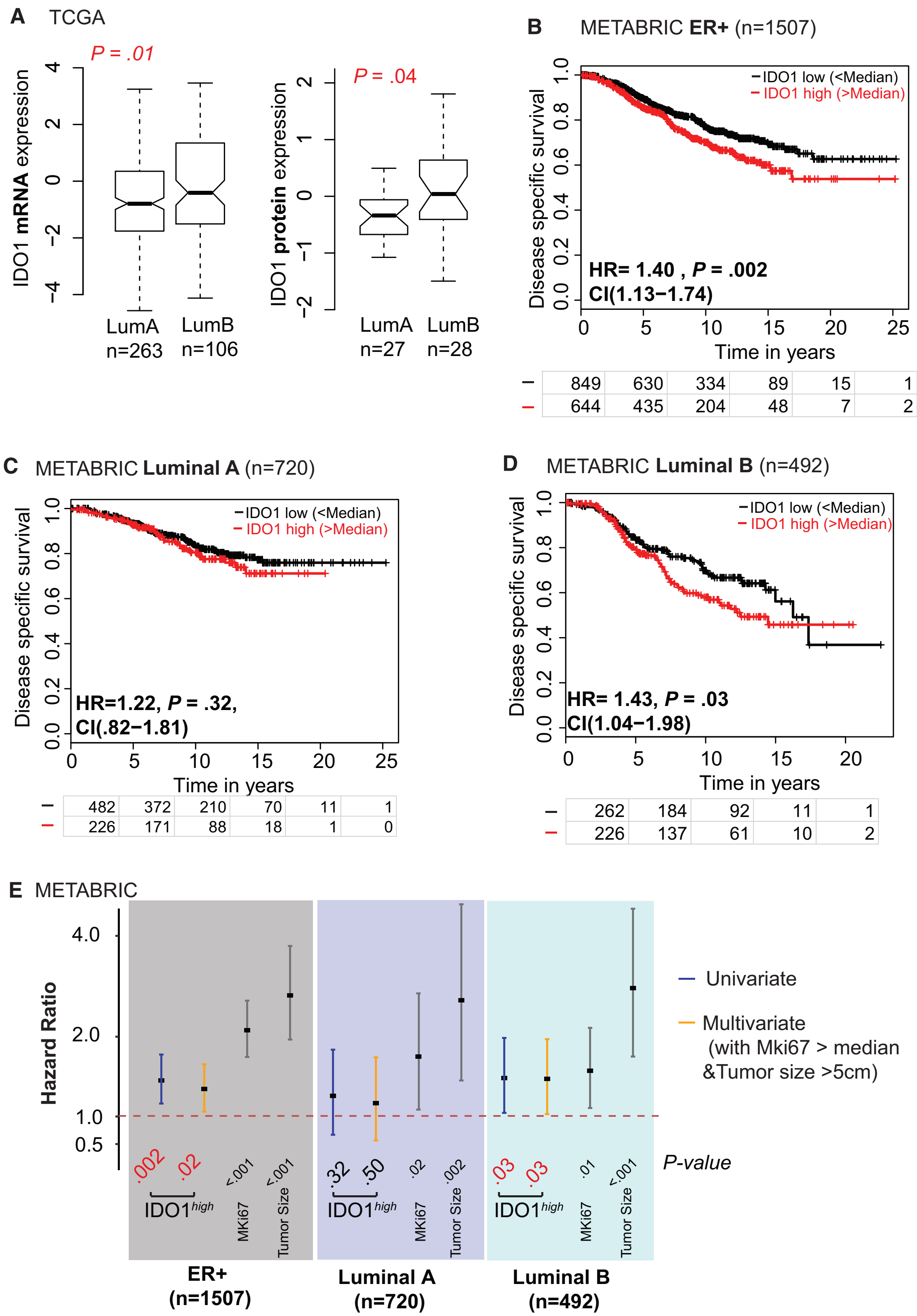

Figure 2. IDO1 levels in Luminal (Lum) B cases. A) Boxplot showing IDO1 protein (left plot) and IDO1 protein levels (right plot) in TCGA LumA and LumB tumors. B) Kaplan-Meier survival curves evaluating disease-specific survival separation based on IDO1 mRNA levels in METABRIC ER-positive breast tumors (n = 1507). C) Kaplan-Meier survival curves evaluating disease-specific survival separation based on IDO1 mRNA levels in METABRIC LumA breast tumors (n = 720). D) Kaplan-Meier survival curves evaluating disease-specific survival separation based on IDO1 mRNA levels in METABRIC LumB breast tumors (n = 492). CI = confidence interval; HR = hazard ratio. Statistically significant *P* values (<.05) are shown in **red**. **Red lines** denote *IDO1*-high cases, and *IDO1*-low cases are shown in **black**. E) Multivariate forest plot of effect of upregulated *IDO1* mRNA levels in METABRIC cohort candidate genes on breast cancer–specific survival when assessed together with other established factors associated with poor prognosis, including high *MKi67* levels and tumor size (>5 cm). Multivariate Cox proportional-hazard model was used in the multivariable analysis. All the tests were two-sided.

ARTICLE

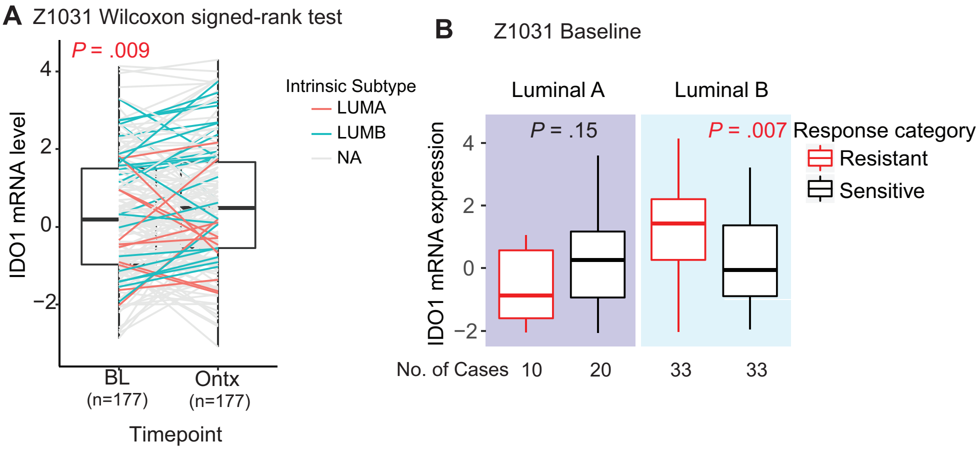

Figure 3. Comparison of IDO1 expression in samples based on treatment timepoint and response to therapy. **A)** Comparison of *IDO1* mRNA expression levels in baseline vs on-treatment estrogen receptor–positive samples. Luminal (Lum) A cases are shown in **teal** and LumB in **orange**. **B)** Boxplot showing *IDO1* expression in tumors categorized based on PAM50 subtype (LumA, LumB) and further separated into endocrine therapy–response categories. Statistical significance was evaluated using Wilcoxon signed-rank and rank-sum tests for matched and independent sample comparisons, respectively. All the tests were two-sided.

IDO1 mRNA levels was independent of Ki67 mRNA levels and tumor size (Figure 2E). The results support the conclusion that the prognostic properties of IDO1 mRNA levels were independent of these proliferation-based biomarkers.

IDO1 Association With Proliferation and Treatment Response

To determine whether IC targets are modulated by ET, we investigated a set of 177 paired samples from Z1031 where baseline and on-treatment microarray expression data were available (Supplementary Table 3, available online). IDO1 mRNA levels were found to increase statistically significantly (baseline median [SD] = 0.19 [1.54] vs on-treatment median [SD] = 0.21 [1.55], $P = .009$) in on-treatment samples (Figure 3A), suggesting that the level of *IDO1* mRNA in the tumor can remain high irrespective of the tumor's responsiveness to neoadjuvant AI. Further categorizing samples based on their PAM50 intrinsic subtype as described by Sorlie et al. (22), *IDO1* mRNA was highest in LumB cases, which failed to respond to ET (Figure 3B; median [SD] LumB sensitive = −0.05 [1.38] vs resistant = 1.42 [1.51], $P = .007$). Further investigation of the association between *IDO1* and on-treatment tumor proliferation (using Ki67 as a marker) demonstrated that *IDO1* mRNA and on-treatment Ki67 showed almost no correlation in LumA tumors (Supplementary Figure 2B, available online), whereas a positive correlation was observed in the LumB cohort ($r = 0.44$; Supplementary Figure 2C, available online).

Correlation Between IDO1 and IFNγ-STAT1 Signaling Pathway in ET-Resistant LumB Breast Cancer

To identify the underlying factors leading to higher *IDO1* levels in ET-resistant LumB cases, we compiled TCGA multi-omics data centered on IDO1. Initially, we investigated amplification at the *IDO1* loci in ER+ breast cancer. However, detailed analyses showed that amplification of *IDO1* did not associate with increased *IDO1* mRNA expression in TCGA ER+ samples (Supplementary Figure 3A, available online). Recent reports suggested methylation-dependent regulation of IDO1 in different cancers. We therefore determined whether hypomethylation was associated with higher IDO1 levels. Though hypomethylation was indeed associated with overexpression of *IDO1* mRNA in ER+ breast cancer (Figure 3B) when cases were categorized based on intrinsic subtypes, this association was statistically significant in the LumA cohort (Supplementary Figure 3C, available online) rather than LumB cohort, suggesting hypomethylation is not the driver for elevated IDO1 expression (Supplementary Figure 3D, available online). We subsequently examined breast cancer data from the CPTAC to identify proteins that correlated with IDO1 [LinkedOmics (16)]. Here STAT1 was found to be ranked second (next to Tryptophanyl-tRNA synthetase) among approximately 700 proteins that positively correlated ($R > 0.4$, $P < .05$) with IDO1 expression (Supplementary Table 4, available online) and (Supplementary Figure 4A, available online). This association was also observed at the STAT1 phospho-protein level (Supplementary Figure 4B, available online).

As expected from the positive correlation expression of *STAT1* followed a similar trend to that of *IDO1*, with enrichment in LumB early-relapse cases (Figure 4A). A similar higher *STAT1* expression was found in resistant LumB cases in the Z1031 mRNA dataset (Figure 4B). No such statistically significant variation in early-relapse or resistant cases was observed in LumA cases in these datasets (Figure 4, A and B), suggesting that LumB tumors might have a specific mechanism for IDO1 overexpression mediated by STAT1. Interestingly, genes associated with higher levels of IDO1 were also associated with IFN-γ hallmark genes (Supplementary Figure 5A, available online). Reanalysis of earlier reported data (23) showed that *IDO1* was the highest upregulated STAT1 target gene in IFN-γ–stimulated HeLa cells [Supplementary Figure 5B (available online), adapted (23)]. An unsupervised clustering of Lum/HER2− cases from the METABRIC patient set based on the mRNA expression of IC genes—*IDO1*, *PD1* (*PDCD1*), and *LAG3*—along with *IFN*γ, *STAT1*, *IRF1*, *MKi67*, and hormone receptor levels, identified a cluster enriched in LumB cases with high levels of IC components and accessory IFNG and STAT1 pathway genes (highlighted in the green box; Figure 4C). *IDO1* clustered tightly with *IFN*γ, along with *PD1*, and *LAG3* clustered with *STAT1*. High-IC samples also showed lower *ER* and *PgR* levels, which is a characteristic of aggressive LumB tumors (24). Based on these immune tolerance genes, a composite immune tolerance score was devised and tested for association with poor prognosis. A high composite immune tolerance score was

ARTICLE

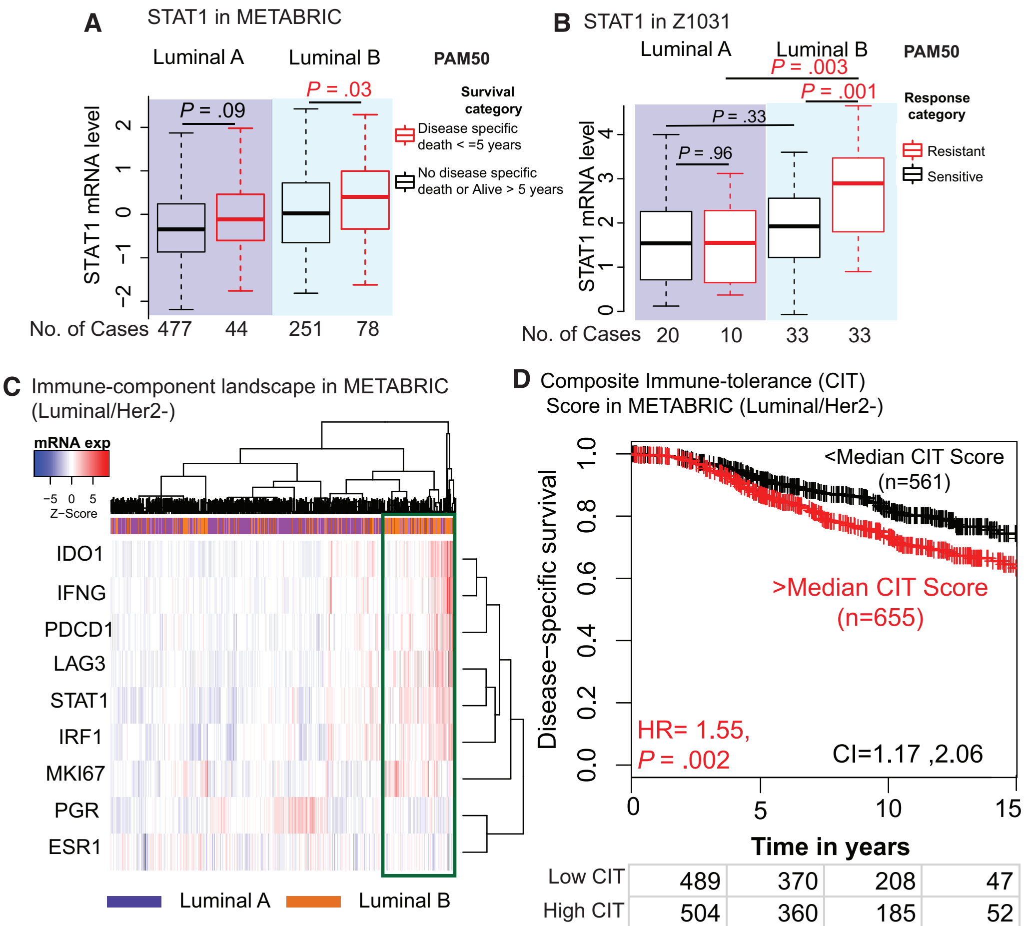

Figure 4. Correlation of *STAT1/IFNG* signaling pathway and immune checkpoint (IC) components in estrogen receptor–positive (ER+) breast cancer. **A, B)** *STAT1* mRNA expression is shown in the Luminal (Lum) A and LumB patient sets, further categorized based on their survival and response category in the METABRIC (A) and Z1031 (B) datasets, respectively. Statistical significance was evaluated using the Wilcoxon rank-sum test. All the tests were two-sided. **C)** Heatmap showing unsupervised clustering of LumA and LumB/*HER2*– cases from the METABRIC patient set based on the mRNA expression of immune checkpoints—IDO1, PD1(PDCD1), and LAG3—along with IFNG, STAT1, IRF1, MKi67, and hormone receptor levels. The **green box** indicates the cluster rich in IC components with high proliferation and low levels of ER and PR. **D)** Kaplan-Meier survival curves evaluating disease-specific survival separation based on immune tolerance score in HER2– luminal cases. CI = confidence interval; HR = hazard ratio. Statistically significant *P* values (<.05) are shown in **red.**

associated with poor DSS in the ER+/HER2– subset of the METABRIC patient cohort (Figure 4D). Similar results were observed in the LumB/HER2– subset of METABRIC (Supplementary Figure 6A, available online) and TCGA (Supplementary Figure 6B, available online).

Association of IDO1 With Clinicopathological Features and Immune Cell Type Composition

The IDO1 association with clinicopathological parameters was further investigated in a Tissue microarray (TMA) analysis of the University of British Columbia (UBC) cohort (see Supplementary Methods, available online, for details) to determine the cell types involved (see Supplementary Methods, available online, on IDO1 staining and immune biomarker scoring). As previously described (25,26), morphologically defined myeloid cells in the stromal compartment not in direct contact with carcinoma cells were distinguished from intraepithelial myeloid cells located within the epithelial carcinoma nests. In these TMA data, IDO1 expression on both intraepithelial and stromal myeloid cells was statistically significantly associated with clinicopathological markers for poor prognosis: high grade, ER negativity, progesterone receptor (PR) negativity, and high Ki67 proliferation index (Table 1). Across all subtypes, cases with IDO1+ intraepithelial myeloid cells were more likely to be LumB and basal-like (38.1% and 33.3%, respectively). As expected based on our mRNA analysis, we report the proportion of breast cancer patients with IDO1+ intraepithelial myeloid cells to be higher in LumB compared with LumA (Table 1; Figure 5B). Subsequent analyses focused on IDO1 associations with the presence of other immune cells, following our previous publications (25,26).

IDO1 expression in intraepithelial myeloid cells was strongly associated with IC markers including PD-L1 expression on carcinoma cells and PD-1 and LAG3 expression on intra-epithelial Tumor infiltrating lymphocytes (TILs) (iTILs; Table 1). We found 25.0% of PD-L1+ tumors, 14.2% of PD-1+ iTILs, and 35.7% of LAG3+ iTILs to be co-infiltrated with IDO1+ intraepithelial myeloid cells. Similarly, IDO1-expressing intraepithelial myeloid cells were statistically significantly associated with the presence of other immune biomarkers, including Foxp3 and CD68 (Table 1). Coinfiltration of lymphocytes carrying Foxp3+ (a

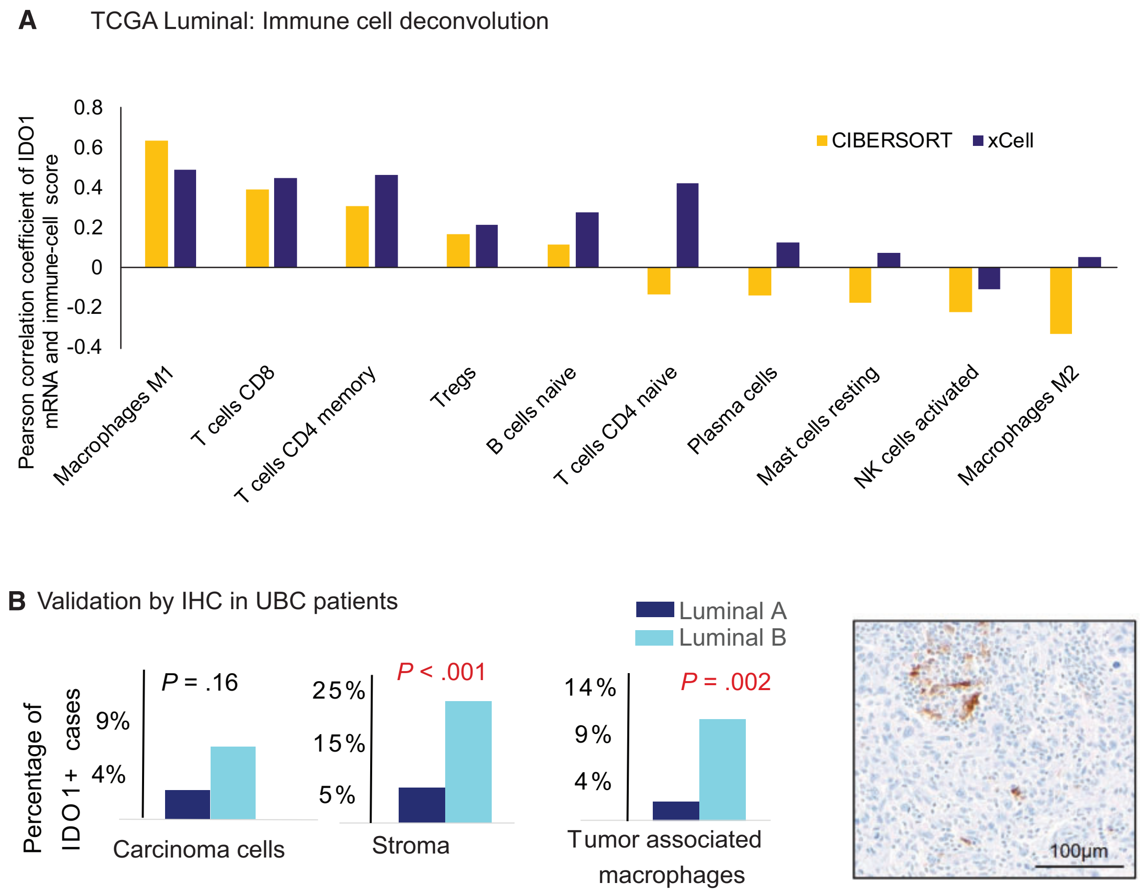

Figure 5. Immune landscape of IDO1-high and endocrine therapy (ET)-resistant disease. A) Histograms represent the correlation between IDO1 mRNA expression and immune cell type scores in the TCGA luminal cohort. Immune cell type correlations obtained from CIBERSORT and xCell are shown in **orange** and **purple**, respectively. B) Histogram showing the percentage of IDO1+ cases (by IHC) in carcinoma cells, stroma, and tumor-associated macrophages along with a representative image of IHC staining in a patient sample. Luminal (Lum) A cases are shown in **blue** and LumB in **teal**. **Scale bar** = 100 µm. Statistical significance was evaluated using two-tailed Fisher exact test.

biomarker for Regulatory T cells [Tregs]) and IDO1+ myeloid cells was observed in 13 cases, which was 100.0% of all IDO1-expressing intraepithelial myeloid cases, or 9.8% of all Foxp3+ iTIL cases (Table 1). In survival analyses of chemotherapy- and/or endocrine-treated breast cancer patients, IDO1+ tumor-associated macrophage cells had no statistically significant associations with DSS (Supplementary Figure 7A, available online). Among the lumB subtype, patients with positive IDO1 expression had a higher percentage of death (50.0%) compared with patients lacking IDO1 expression (20.0%; Supplementary Figure 7C, available online), a difference not observed with the LumA subtype (Supplementary Figure 7B, available online). However, neither difference was statistically significant, likely because of a limited sample size.

Furthermore, 76.9% of IDO1-expressing intraepithelial myeloid cases were coinfiltrated with macrophages (identified as CD68+, $P = .02$; Table 1). No statistically significant co-infiltration was observed with M2 macrophages (identified as CD163+). In TMA analysis, IDO1 showed statistically significant association with all macrophages but not specifically with M2, suggesting that the association is associated with either macrophage M0 or M1. Because there is no specific IHC biomarker for M1 macrophages, further granularity cannot be obtained at the IHC level. To overcome this limitation, we investigated *IDO1* association with different immune cell types based on CIBERSORT and xCell categorization and scores. *IDO1* mRNA showed the strongest (by CIBERSORT) correlation with macrophage M1 at the mRNA level (Figure 5A), which agrees with earlier published reports on IFN-γ–dependent upregulation of IDO1 and differentiation of THP-1 monocyte cells to M1 macrophages (27). Collective observations from IHC and mRNA suggest that *IDO1* expression associates with Tregs and macrophages (particularly M1 based on CIBERSORT analysis).

To identify and verify sites of IDO1 expression, IHC staining of a TMA of 330 cases of a diverse spectrum of breast cancer samples was employed. Here we observed higher IDO1+ staining in stroma ($P < .001$) and tumor-associated macrophages ($P = .02$) in LumB cases (22.97% and 6.76%, respectively) compared with LumA counterparts (6.67% and 2.67%, respectively) (Figure 5B).

Discussion

High levels of IC components associate with poor prognosis in many cancers (28–31). In breast cancer, expression of ICs including PD1 and IDO1 has been associated primarily with metastatic or triple-negative breast cancers (32), and the immune environment of the ER+ subset is understudied. This is primarily because ER+ tumors have been considered to be immunologically “cold” because of low TIL counts (33). Although this is true for

Table 1. Association of IDO1+ intraepithelial cells with clinicopathological parameters and immune biomarkers in UBC cohort and ER+ subset of the UBC cohort

Clinicopathological parameters	IDO1+ myeloid = 0 (n = 277), No. (%)	IDO1+ myeloid positive (≥1) (n = 29), No. (%)	P*
All subtypes (UBC cohort)			
Grade			<.001
1 or 2	162 (59.6)	7 (24.1)	
3	110 (40.4)	22 (75.9)	
ER			<.001
Negative	48 (17.6)	16 (55.2)	
Positive	225 (82.4)	13 (44.8)	
PR			.002
Negative	80 (29.6)	17 (58.6)	
Positive	190 (70.4)	12 (41.4)	
Ki67			<.001
<13.25%	161 (59.9)	4 (13.8)	
≥13.25%	108 (40.1)	25 (86.2)	
Subtype			<.001
Luminal A	146 (60.1)	4 (19.0)	
Luminal B	66 (27.2)	8 (38.1)	
HER2+	9 (3.7)	2 (9.5)	
Core basal	22 (9.1)	7 (33.3)	
ER-positive subset (UBC cohort)			
PD1+ iTILs			<.001
Negative	177 (85.5)	3 (23.1)	
Positive	30 (14.5)	10 (76.9)	
PDL1			.25
Negative	185 (96.9)	9 (90.0)	
Positive	6 (3.1)	1 (10.0)	
LAG3+ iTILs			<.001
Negative	181 (95.3)	5 (50.0)	
Positive	9 (4.7)	5 (50.0)	
CD8+ iTILs			.27
Negative	72 (40.7)	2 (22.2)	
Positive	105 (59.3)	7 (77.8)	
Foxp3+ iTILs			.002
Negative	91 (43.3)	0 (0.0)	
Positive	119 (56.7)	13 (100)	
CD163 intraepithelial			.22
Negative	202 (93.5)	11 (84.6)	
Positive	14 (6.5)	2 (15.4)	
CD68 intraepithelial			.02
Negative	117 (56.0)	3 (23.1)	
Positive	92 (44.0)	10 (76.9)	

*P values were calculated using a two-sided χ^2 test. All the tests were two-sided.

the majority of ER+ tumors (primarily LumA disease), almost no study so far has focused on more aggressive LumB cases. However, a recent report indicated that high TIL levels are associated with higher recurrence scores in ER+ tumors (34). It is important to report that our present study was not initially focused on IC components but rather with an unbiased genome-wide profiling analysis to identify genes that are upregulated in ET-resistant tumors. Our results highlight the role of upregulated ICs leading to a higher degree of immune tolerance in a subset of LumB tumors. High IDO1 levels showed a statistically significant association with poor prognosis in LumB breast cancer. There have been contrary reports of better overall survival in ER+ patients with high IDO expression as measured by IHC (35). However, in these studies, the majority of the reported ER+ tumors were classified as LumA, whereas this study uncovered a consistent phenomenon of *IDO1* upregulation specifically in LumB tumors. Though the patient size is modest in our discovery dataset (n = 66 for LumB), further validation of the findings in two independent patient cohorts, TCGA (n = 91) and METABRIC (n = 492), addresses this shortcoming. We do acknowledge the need for sequencing data from a larger cohort of ER+ patients, and the ALTERNATE trial, which has now completed accrual of more than 1400 cases, presents an upcoming opportunity to do this (36).

Interestingly, associations between *IDO1* expression levels and outcome have been reported in other cancer types with apparently inconsistent results. For example, higher IDO1 levels correlate with poor survival in glioblastoma patients (TCGA) in contrast to the correlation observed between increased *IDO1* levels and better overall survival in melanoma patients (20). These tumors have very different etiologies and mutational mechanisms, and so the influence of IDO1 may well be tumor specific or in our case breast cancer subtype specific. There have been recent indications of dual roles for IDO1 depending on its localization in the tumors. This discordance could be influenced by the type of cells expressing high levels of IDO1. For instance, in this study, we observed higher IDO1+ staining in stroma and particularly in tumor-associated macrophages compared with carcinoma cells. Interestingly, we observed a strong association between tumors infiltrated with CD8+ T-cells and IDO1+ myeloid cells, suggesting potential exhaustion of CD8+ T-cells by overexpression of IDO1 and suppression of antitumor cytotoxic T-cell activity.

Our study also suggests an association between IDO1 and both macrophages and T-regs. Classification of macrophages is complicated, but according to CIBERSORT, they comprise three types: macrophage 0 (uncommitted), 1 (classically activated), and 2 (alternatively activated) (37). *IDO1* mRNA expression associated strongly with CIBERSORT-based M1 macrophages score. We are aware that recent studies suggest the M1-M2 macrophage model may be oversimplified (38).

It is worth noting that selected ICs were found to be upregulated in a small subset of ER+ cases; hence, drug targeting ICs in nonstratified ER+ patient populations risks clinical trial failure. For example, the inactivity of epacadostat (an IDO1 inhibitor) in initial trials does not necessarily mean IDO1 is a poor therapeutic target (39); rather, it may signify the importance of patient stratification and tailoring of therapeutics based on molecular insights. The results from this study provide a strong rationale for clinical trials of IC inhibitors in aggressive ER+ breast cancers, particularly LumB cases that fail to respond to neoadjuvant ET.

Our study has limitations. Though we attempted to capture evidence for IC activity in ER+ breast cancer at the multi-omics and TMA levels, we acknowledge that mRNA, methylation, and IHC assessments can be affected by intratumoral heterogeneity, which means tumors can be incorrectly assigned to the wrong biomarker class. Our study does not directly address this concern; however, we have focused on findings that can be replicated in multiple independent studies, thereby suggesting the rate of incorrect assignment is low enough for the results to be consistent (40).

To summarize, this study is a step forward from our earlier published work, which identified dysregulation of single-strand break repair genes as being causal to ET resistance. We report upregulation of IC components, including IDO1 and LAG3, in ET-resistant LumB tumors. This presents new information on the role of the immune microenvironment in poor-prognosis ER+ breast cancer and suggests strategies to engage antitumor

CD8+ T cells to improve patient outcomes. These data also serve as a useful guide for mechanistic studies to improve our understanding of IC components and immune tolerance in ET-resistant LumB tumors.

Funding

Research reported in this publication was primarily supported by a Susan G. Komen Promise grant (PG12220321), a Cancer Prevention and Research Institute of Texas (CPRIT) "Recruitment of Established Investigators" award (RR140033), and CPTAC (U01CA214125 to MJE). MJE is a CPRIT scholar in cancer research, a McNair Foundation scholar at Baylor College of Medicine, and Susan G. Komen Scholar (SAC170059) and mentor (CCR18548157) in breast cancer research. Clinical trial data accrual and sample analysis were supported by the National Cancer Institute of the NIH under award numbers U10CA180821, U10CA180882, and U24CA196171 (to the Alliance for Clinical Trials in Oncology) as well as R01 CA095614, U10CA180833, and U10CA180858. The Z1031 trial was also supported, in part, by funds from AstraZeneca, Novartis Pharmaceutical Corporation, and Pfizer, Inc. Research is also supported by NCI CPTAC grant (U24CA210954) and CPRIT award (RR160027) to BZ, who is a CPRIT Scholar in Cancer Research and a McNair Scholar.

Notes

Author affiliations: Lester and Sue Smith Breast Center (MA, CH, SV, JW, XHZ, BZ, MJE) and Department of Medicine (MA, JW, MJE), Baylor College of Medicine, Houston, TX; Genetic Pathology Evaluation Centre (MZ, SB, DG, TN) and Pathology and Laboratory Medicine Department (MZ, SB, DG, TN), University of British Columbia, Vancouver, BC; Department of Molecular and Human Genetics (CH, SV, XHZ, BZ) and Department of Molecular and Cellular Biology (JW), Baylor College of Medicine, Houston, TX; Siteman Cancer Center Breast Cancer Program, Washington University School of Medicine, Saint Louis, MO (JH); Alliance Statistics and Data Center, Mayo Clinic, Rochester, MN (VS). Department of Translational Molecular Pathology, The University of Texas MD Anderson Cancer Center, Houston, TX (SV).

The content is solely the responsibility of the authors and does not necessarily represent the official views of the National Institutes of Health. The funders had no role in the design of the study; the collection, analysis, and interpretation of the data; the writing of the manuscript; and the decision to submit the manuscript for publication.

M. J. Ellis and T. O. Nielsen hold ownership interests (including patents) in Bioclassifier LLC relating to the PAM50 test, which has been licensed to NanoString Technologies. M. J. Ellis is a consultant or advisory board member for NanoString, Pfizer, Novartis, and AstraZeneca. No potential conflicts of interest were disclosed by the other authors.

The authors acknowledge Drs S. M. Kavuri, Eric Chang, Susan Hilsenbeck, Kimberly Holloway, Jonathan T. Lei, and Svasti Haricharan for their scientific input. The authors thank Dr Gary C. Chamness for critical reading of the manuscript. Authors also acknowledge and thank Alliance for Clinical Trials in Oncology for their support.

References

1. Metzger-Filho O, Sun Z, Viale G, et al. Patterns of recurrence and outcome according to breast cancer subtypes in lymph node-negative disease: results from International Breast Cancer Study Group Trials VIII and IX. *J Clin Oncol*. 2013;31(25):3083–3090.
2. Smith IE, Dowsett M. Aromatase inhibitors in breast cancer. *N Engl J Med*. 2003;348(24):2431–2442.
3. Coleman RE. Current and future status of adjuvant therapy for breast cancer. *Cancer*. 2003;97(3 Suppl):880–886.
4. Carpenter R, Miller WR. Role of aromatase inhibitors in breast cancer. *Br J Cancer*. 2005;93(Suppl 1):S1–S5.
5. Ellis MJ, Suman VJ, Hoog J, et al. Ki67 proliferation index as a tool for chemotherapy decisions during and after neoadjuvant aromatase inhibitor treatment of breast cancer: results from the American College of Surgeons Oncology Group Z1031 Trial (Alliance). *JCO*. 2017;35(10):1061–1069.
6. O'Leary B, Cutts RJ, Liu Y, et al. The genetic landscape and clonal evolution of breast cancer resistance to palbociclib plus fulvestrant in the PALOMA-3 trial. *Cancer Discov*. 2018;8(11):1390–1403.
7. Razavi P, Chang MT, Xu G, et al. The genomic landscape of endocrine-resistant advanced breast cancers. *Cancer Cell*. 2018;34(3):427–438.e6.
8. Haricharan S, Punturi N, Singh P, et al. Loss of MutL disrupts CHK2-dependent cell-cycle control through CDK4/6 to promote intrinsic endocrine therapy resistance in primary breast cancer. *Cancer Discov*. 2017;7(10):1168–1183.
9. Anurag M, Punturi N, Hoog J, et al. Comprehensive profiling of DNA repair defects in breast cancer identifies a novel class of endocrine therapy resistance drivers. *Clin Cancer Res*. 2018;24(19):4887–4899.
10. Andor N, Maley CC, Ji HP. Genomic instability in cancer: teetering on the limit of tolerance. *Cancer Res*. 2017;77(9):2179–2185.
11. Wang J, Duncan D, Shi Z, et al. WEB-based GEne SeT AnaLysis toolkit (WebGestalt): update 2013. *Nucleic Acids Res*. 2013;41(Web Server issue): W77–W83.
12. Wang J, Vasaikar S, Shi Z, et al. WebGestalt 2017: a more comprehensive, powerful, flexible and interactive gene set enrichment analysis toolkit. *Nucleic Acids Res*. 2017;45(W1):W130–W137.
13. Kaplan EL, Meier P. Nonparametric estimation from incomplete observations. *J Am Stat Assoc*. 1958;53(282):457–481.
14. Cox DR. Regression models and life-tables. *J R Stat Soc Series B Stat Methodol*. 1972;34(2):187–220.
15. Diez-Villanueva A, Mallona I, Peinado MA. Wanderer, an interactive viewer to explore DNA methylation and gene expression data in human cancer. *Epigenetics Chromatin*. 2015;8:22.
16. Vasaikar SV, Straub P, Wang J, et al. LinkedOmics: analyzing multi-omics data within and across 32 cancer types. *Nucleic Acids Res*. 2018;46(D1): D956–D963.
17. Edwards NJ, Oberti M, Thangudu RR, et al. The CPTAC data portal: a resource for cancer proteomics research. *J Proteome Res*. 2015;14(6):2707–2713.
18. Anurag M, Ellis MJ, Haricharan S. DNA damage repair defects as a new class of endocrine treatment resistance driver. *Oncotarget*. 2018;9(91): 36252–36253.
19. Naidoo J, Page DB, Li BT, et al. Toxicities of the anti-PD-1 and anti-PD-L1 immune checkpoint antibodies. *Ann Oncol*. 2015;26(12):2375–2391.
20. Zhai L, Ladomersky E, Lenzen A, et al. IDO1 in cancer: a Gemini of immune checkpoints. *Cell Mol Immunol*. 2018;15(5):447–457.
21. Mertins P, Mani DR, Ruggles KV, et al. Proteogenomics connects somatic mutations to signalling in breast cancer. *Nature*. 2016;534(7605):55–62.
22. Sorlie T, Tibshirani R, Parker J, et al. Repeated observation of breast tumor subtypes in independent gene expression data sets. *PNAS U S A*. 2003;100(14): 8418–8423.
23. Satoh J, Tabunoki H. A comprehensive profile of ChIP-Seq-based STAT1 target genes suggests the complexity of STAT1-mediated gene regulatory mechanisms. *Gene Regul Syst Biol*. 2013;7:41–56.
24. Maisonneuve P, Disalvatore D, Rotmensz N, et al. Proposed new clinicopathological surrogate definitions of luminal A and luminal B (HER2-negative) intrinsic breast cancer subtypes. *Breast Cancer Res*. 2014; 16(3):R65.
25. Liu S, Foulkes WD, Leung S, et al. Prognostic significance of FOXP3+ tumor-infiltrating lymphocytes in breast cancer depends on estrogen receptor and human epidermal growth factor receptor-2 expression status and concurrent cytotoxic T-cell infiltration. *Breast Cancer Res*. 2014;16(5):432.
26. Burugu S, Gao D, Leung S, et al. LAG-3+ tumor infiltrating lymphocytes in breast cancer: clinical correlates and association with PD-1/PD-L1+ tumors. *Ann Oncol*. 2017;28(12):2977–2984.
27. Wang XF, Wang HS, Wang H, et al. The role of indoleamine 2, 3-dioxygenase (IDO) in immune tolerance: focus on macrophage polarization of THP-1 cells. *Cell Immunol*. 2014;289(1–2):42–48.
28. Brandacher G, Perathoner A, Ladurner R, et al. Prognostic value of indoleamine 2, 3-dioxygenase expression in colorectal cancer: effect on tumor-infiltrating T cells. *Clin Cancer Res*. 2006;12(4):1144–1151.
29. Giraldo NA, Becht E, Pages F, et al. Orchestration and prognostic significance of immune checkpoints in the microenvironment of primary and metastatic renal cell cancer. *Clin Cancer Res*. 2015;21(13):3031–3040.
30. Uso M, Jantus-Lewintre E, Calabuig-Farinas S, et al. Analysis of the prognostic role of an immune checkpoint score in resected non-small cell lung cancer patients. *Oncoimmunology*. 2017;6(1):e1260214.
31. Yao J, Xi W, Zhu Y, et al. Checkpoint molecule PD-1-assisted CD8(+) T lymphocyte count in tumor microenvironment predicts overall survival of

patients with metastatic renal cell carcinoma treated with tyrosine kinase inhibitors. *CMAR*. 2018;10:3419–3431.
32. Dill EA, Dillon PM, Bullock TN, et al. IDO expression in breast cancer: an assessment of 281 primary and metastatic cases with comparison to PD-L1. *Mod Pathol*. 2018;31(10):1513–1522.
33. Loi S, Sirtaine N, Piette F, et al. Prognostic and predictive value of tumor-infiltrating lymphocytes in a phase III randomized adjuvant breast cancer trial in node-positive breast cancer comparing the addition of docetaxel to doxorubicin with doxorubicin-based chemotherapy: BIG 02-98. *J Clin Oncol*. 2013;31(7):860–867.
34. Ahn SG, Cha YJ, Bae SJ, et al. Comparisons of tumor-infiltrating lymphocyte levels and the 21-gene recurrence score in ER-positive/HER2-negative breast cancer. *BMC Cancer*. 2018;18(1):320.
35. Soliman H, Rawal B, Fulp J, et al. Analysis of indoleamine 2-3 dioxygenase (IDO1) expression in breast cancer tissue by immunohistochemistry. *Cancer Immunol Immunother*. 2013;62(5):829–837.
36. Suman VJ, Ellis MJ, Ma CX. The ALTERNATE trial: assessing a biomarker driven strategy for the treatment of post-menopausal women with ER+/Her2- invasive breast cancer. *Chin Clin Oncol*. 2015;4(3):34.
37. Tarique AA, Logan J, Thomas E, et al. Phenotypic, functional, and plasticity features of classical and alternatively activated human macrophages. *Am J Respir Cell Mol Biol*. 2015;53(5):676–688.
38. Azizi E, Carr AJ, Plitas G, et al. Single-cell map of diverse immune phenotypes in the breast tumor microenvironment. *Cell*. 2018;174(5):1293–1308.e36.
39. Zhu MMT, Dancsok AR, Nielsen TO. Indoleamine dioxygenase inhibitors: clinical rationale and current development. *Curr Oncol Rep*. 2019;21(1):2.
40. Thorsson V, Gibbs DL, Brown SD, et al. The immune landscape of cancer. *Immunity*. 2018;48(4):812–830.e14.

ARTICLE